Absolute total and partial cross sections for the electron impact ionization of tetrafluorosilane (SiF_4)

R. Basner,[a] M. Schmidt, and E. Denisov
Institut für Niedertemperatur-Plasmaphysik, Friedrich-Ludwig-Jahn-Strasse 19, D-17489 Greifswald, Germany

K. Becker
Department of Physics and Engineering Physics, Stevens Institute of Technology, Hoboken, New Jersey 07030

H. Deutsch
Institut für Physik, Ernst-Moritz-Arndt-Universität, Domstrasse 10a, D-17487 Greifswald, Germany

(Received 11 August 2000; accepted 24 October 2000)

We measured absolute partial cross sections for the formation of various singly charged and doubly charged positive ions produced by electron impact on SiF_4 from threshold to 900 eV using a time-of-flight mass spectrometer. Dissociative ionization was found to be the dominant process, although we found evidence of the presence of the SiF_4^+ parent ion in our experiment. The SiF_3^+ fragment ion has the largest partial ionization cross section with a maximum value of $4.3 \times 10^{-16}\,cm^2$ at 90 eV. All other singly charged fragment ion cross sections are about one order of magnitude smaller at this impact energy. The cross-section values of the doubly charged ions with the exception of SiF_2^{++} are about two orders of magnitude smaller. A comparison is made with available previously measured data. Additional measurements using a sector-field mass spectrometer revealed that all fragment ions are formed with excess kinetic energy. The experimentally determined total single ionization cross section of SiF_4 is compared with results of semiempirical and semiclassical calculations and reasonable agreement is found. © *2001 American Institute of Physics.* [DOI: 10.1063/1.1333018]

I. INTRODUCTION

Low-temperature fluorine-based plasmas have been successfully used for plasma-assisted etching and deposition of silicon layers in the fabrication of microelectronic devices and solar cells. Tetrafluorosilane (SiF_4) and the SiF_x ($x=1-3$) free radicals play an important role in these plasmas. Highly reactive fluorine atoms and ions from the plasma interact with the substrate or surface and produce volatile reaction products, primarily SiF_4 and SiF_2.[1–5] These reaction products, in turn, diffuse back into the plasma where they are dissociated and ionized by the plasma electrons and the resultant products are transported and redeposited onto the substrate and/or surface. SiF_4 is used also in the plasma-assisted deposition of thin silicon films.[6,7] Thus, electron-impact cross sections for the dissociation and ionization of SiF_4 and the SiF_x ($x=1-3$) radicals are important quantities in efforts to understand and model the silicon–fluorine plasma-surface chemistry.

Previous work on electron interactions with SiF_x ($x=1-4$) include the ionization cross-section measurements of the three radicals SiF, SiF_2, and SiF_3 by Freund and co-workers[8–10] as well as the ionization cross-section measurement for the Si atom.[11] Poll and Meichsner[12] reported a SiF_3^+ partial ionization cross section following electron impact ionization of SiF_4 measured by using a quadrupole mass spectrometer. Nakano and Sugai[13] used this result for the calibration of their measured relative ionization curves to give absolute partial ionization cross sections of the ions SiF_4^+, SiF_2^+, and SiF^+ in the energy range from threshold to 60 eV. To date, these are the only published partial ionization cross-section measurements for the SiF_4 molecule. We note that both measurements were taken with quadrupole mass spectrometers, which are known to have a mass-dependent transmission. Nakano and Sugai[13] also reported absolute cross sections for the electron-impact dissociation of SiF_4 into neutral fragments (SiF_3, SiF_2, SiF, and Si) using threshold ionization mass spectrometry. More recently, Becker and co-workers have studied the formation of final-state specific Si(^1S) atoms following electron-impact dissociation of SiF_4.[14] Other available data for SiF_4 include total electron scattering cross sections,[15] vibrational excitation,[16] UV emission[17] and formation of negative ions[18] induced by electron impact, photoabsorption, photoionization, and fluorescence cross sections,[19–22] the cross section for the reaction of Si^+,[23] and N^+, N_2^+, Ar^+, Kr^+[24] with SiF_4, molecular orbital studies of the thermal decomposition of SiF_4,[25] and soft x-ray photochemistry of physisorbed SiF_4.[26,27]

In this paper we report experimental results of absolute partial and total electron impact ionization cross sections of SiF_4, including all singly charged positive ions SiF_x^+ ($x=1-4$), Si^+, F^+, and the doubly charged ions SiF_x^{++} ($x=1-3$), and Si^{++}. The total ionization cross section is obtained as the sum of the partial cross sections. The total single ionization cross section is compared with results of the semiclassical and semiempirical calculations and reasonable

[a]Electronic mail: basner@inp-greifswald.de

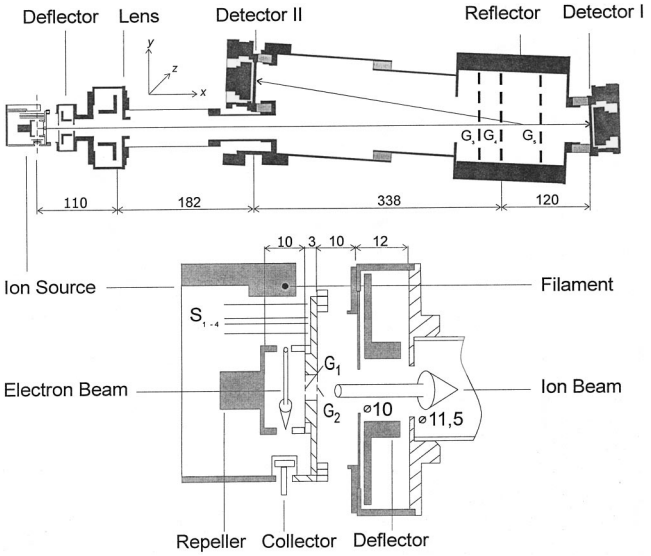

FIG. 1. Schematic diagram of the time-of-flight mass spectrometer and a detailed view of the electron impact ion source used in the present study (all dimensions are in mm): electron beam [tungsten filament, 0—(−900) V]; apertures: S_1 (0.5×4 mm^2, 22.4 V preacceleration), S_2/S_3 (0.5×4 mm^2, 22.4 or 70 V below the potential of the filament, pulsed), S_4 (0.4×0.4 mm^2, grounded); repeller ($0-\pm3$ kV); collision chamber exit aperture (6.5×6.5 mm^2, molybdenum grids (G_1,G_2): transmission 90%, grounded); flight tube entrance electrode (diameter 10 mm, $0-\pm3$ kV); deflector ($0-\pm500$ V); Einzel lenses ($0-\pm13$ kV); reflector [copper grids (G_3,G_4,G_5): transmission 94%]; detectors I and II (Galileo, 40-mm-diam MCP, active area 12.5 cm^2).

agreement is found. This is a continuation of our activities in the field of measurements of electron impact ionization cross sections of molecules and radicals which are important for plasma processing.[28–35]

II. EXPERIMENTAL APPARATUS

The measurements were carried out using a time-of-flight mass spectrometer (TOFMS). Ma *et al.*[36] and subsequently Straub *et al.*[37] first described the application of the time-of-flight technique to absolute partial ionization cross-section measurements. Our apparatus is shown schematically in Fig. 1. It consists of two interconnected stainless steel vacuum chambers that are evacuated separately by two turbomolecular pumps to a base pressure of 1×10^{-6} Pa. One chamber contains the electron-impact ion source and the other chamber houses the ion flight tube and the ion detectors. The TOFMS can be operated either in a linear mode using detector I or in a reflection mode using the reflector (grids: G_3, G_4, G_5 made from copper with 94% optical transmission) and detector II. Both detectors are microchannel plate detectors (MCP, dual-plate chevron arrangement, Galileo Electro-Optics Corp.) of 40 mm diameter. In the present study, all measurements were performed with the TOFMS operated in the linear mode to ensure complete ion transport from the ion source to the detector. The ion source chamber was filled with the target gas under study at pressures of about 1×10^{-4} Pa, which is measured with a spinning rotor viscosity gauge. Argon, which is used as reference gas, was always added to the ion source for test and calibration purposes. The ion efficiency curves (relative partial ionization cross sections) were measured simultaneously for Ar and SiF_4 in a well-defined SiF_4/Ar mixture in an effort to ensure identical operating conditions for the detection of the ions from SiF_4 and the Ar^+ and Ar^{++} ions. The measured relative partial ionization cross sections were put on an absolute scale by normalization relative to the total Ar ionization cross section of 2.77×10^{-16} cm^2 at 70 eV.[38] Taking into account the uncertainties of $\pm7\%$ in the Ar reference cross section,[36] the statistical uncertainty in our pressure measurement of $\pm3\%$, and the counting statistics of $\pm5\%$ we assign an overall uncertainty of about $\pm15\%$ to the absolute ionization cross sections reported here.

Typically, the electron gun was operated using electron pulses of 90 ns width at a repetition rate of 15 kHz. The electron beam has a diameter of about 0.6 mm in the interaction region and the dc-equivalent electron beam current is in the range from 1–10 μA with an energy spread of about 0.5 eV (full width at half maximum). The impact energy was varied from 5 to 900 eV and the electron beam is guided by a weak magnetic field (200 G). Voltages up to 3 kV (extraction fields up to 3 kV cm^{-1}) with a 10 ns rise time are applied to the repeller roughly 10 ns after the incident electron pulse has passed through the ionization region. This extraction pulse accelerates the ions formed by electron impact toward the grounded ion source exit aperture. After passing through the exit aperture (grids: G_1, G_2 made from molybdenum with 90% optical transmission) the ions are accelerated by a -3 kV bias voltage applied to the entrance electrode of the flight tube. The ion deflector section consists of two pairs of electrodes for the deflection of the ions in the horizontal (z) and vertical (y) directions. The deflection plates in conjunction with the Einzel lens allow corrections of the ion trajectories. The first detector arrangement (detector I) is placed at the end of the flight tube. When the TOFMS is operated in the reflection mode with much higher mass resolution ($m/\Delta m=1500$ as compared to a mass resolution of about 50 in the linear mode), the three additional grids G_3, G_4, G_5 are employed to reverse the direction of the ions which are then detected by the second detector arrangement (detector II). The output from the MCP is preamplified and recorded with a 2 GHz multiscaler (FAST ComTec, Model 7886) with a time resolution of 500 ps. Our TOFMS was operated in such a way that no more than one ion is created during each electron pulse. This results in low overall count rates and comparatively long data acquisition times, but ensures, on the other hand, that dead time corrections to the recorded signal rates are negligible. We further maintained operating conditions under which the ion count rate varied linearly with the gas pressure and the electron beam current.

Fragment ions resulting from the dissociative ionization of a molecule are often formed with excess kinetic energies, which can interfere with the complete extraction and transmission of the ions from the interaction region to the detector. We found that fragment ions of SiF_4 are generally formed with significant excess kinetic energies (see results in the following). In our experiment the excess kinetic energy leads to the following effects:

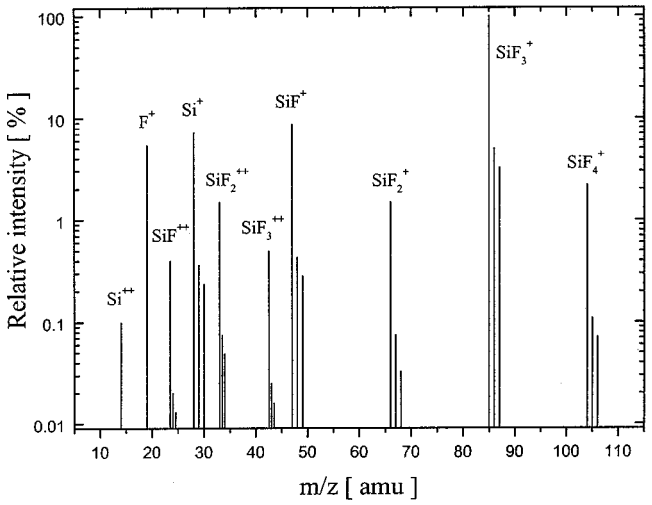

FIG. 2. Mass spectrum of SiF_4 at 70 eV impact energy measured with the time-of-flight mass spectrometer in the linear mode.

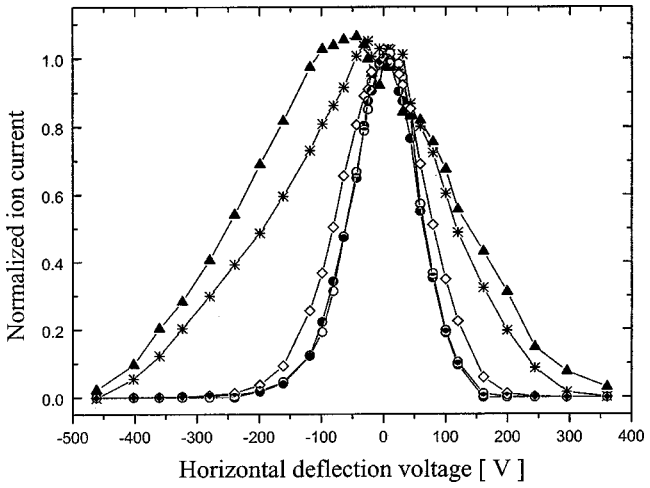

FIG. 3. Normalized ion beam currents of the ions SiF_4^+ (closed circles), SiF_3^+ (open diamonds), SiF^+ (closed triangles), Si^+ (stars), and Ar^+ (open circles) as a function of the horizontal deflection voltage at 70 eV impact energy. These data were obtained with a double-focusing sector-field mass spectrometer using a modified ion extraction stage (Refs. 32 and 33).

(i) The ion source region, which is normally determined by the spatial dimensions of the electron beam, is enlarged because of the motion of the ions during the time interval between their formation and their extraction.

(ii) The divergence of the extracted ''ion beam'' is enlarged both spatially as well as temporally due to the variation in the spatial positions, momenta, and energies of the ions when the extraction pulse is applied.

Measurements of the ion extraction efficiency as a function of the delay time between the end of the electron pulse and the beginning of the extraction pulse to the repeller revealed constant ion currents for all fragment ions of SiF_4 as long as the delay times were below 50 ns. This indicates that all ions from the extraction region of the ion source are transported to the detector under these conditions. Furthermore, extensive studies varying the voltages on the Einzel lens and on the horizontal and vertical deflection plates ensured that the diameter of the ''ion beam'' at the end of the flight tube is smaller than the diameter of the MCP (40 mm) for every fragment ion. We conclude that the experimental conditions necessary for 100% ion transmission of the ions from the ion source to the detector were established with the exception of ion loss at the grids G_1 and G_2. Moreover, we found no evidence for instability of the SiF_4^+ molecular ion in the period from 1×10^{-7} to 1×10^{-5} s after their formation by changing the flight time at our experiment.

Since our technique relies on measurements of ratios of ions, the detection efficiency of the MCP for the reference ion and the various product ions of the gas under study must be the same. A series of experiments was performed to measure the ion count rate of a constant incident ion flux as a function of the ion impact energy for given operating voltages of the MCP and threshold levels of the multiscaler. Increasing the ion energy and the operating voltage of the MCP while decreasing the threshold level of the multiscaler revealed a saturation value of the recorded ion count rate. The saturation for doubly charged ions at the same ion impact energy always occurred at a lower operating voltage of the MCP as expected. Optimum operating conditions were found for voltages of 2 kV across both channel plates with a voltage difference of 300 V between the last plate and the anode. A minimum threshold level of the multiscaler well above the noise level was selected in such a way that the ion count rate was saturated for all singly charged ions with ion impact energies higher than 3.2 keV (0.5 keV from the extraction and 2.7 keV from the acceleration) and for all doubly charged ions with twice the ion impact energies. Under these conditions, we measured the double-to-single ionization cross-section ratio in Ar (Ar^{++}/Ar^+) at 100 eV electron energy to be 0.073 ± 0.005, which is in excellent agreement with the most reliable values reported in the literature.[37,39,40] We assume that the ion impact energy is high enough to guarantee a 100% counting efficiency for each ion hitting the front channel plate.

In the linear mode of the TOFMS, the mass resolution is sufficient to separate the signals arising from the different ions, but it is not sufficient to resolve the signals attributed to the various isotopes of the heavier Si-containing ions. Thus we summed the ion counts corresponding to the three Si isotopes, ^{28}Si (92.3%), ^{29}Si (4.7%), and ^{30}Si (3.0%).

III. RESULTS AND DISCUSSIONS

The mass spectrum of SiF_4 is shown in Fig. 2 using a logarithmic scale for the relative intensities. It was derived from measurements carried out with the TOFMS operated in the linear mode at an electron energy of 70 eV. A very small background correction was applied to the spectrum because of the presence of trace concentrations of OH, H_2O, N_2, and O_2 in the background gas. The spectrum shows some noteworthy differences compared with the spectra found in mass spectrometric databases,[41–43] particularly in the range of

TABLE I. Absolute partial (counting) and total (charge weighted) electron impact ionization cross sections (10^{-16} cm^2) for SiF_4 as a function of electron energy from threshold to 900 eV.

Electron energy (eV)	Ion						Electron energy (eV)	Ion					
	SiF_4^+	SiF_3^+	SiF_2^+	SiF^+	Si^+	F^+		SiF_4^+	SiF_3^+	SiF_2^+	SiF^+	Si^+	F^+
16	0.003						54	0.083	3.61	0.055	0.280	0.177	0.097
17	0.006	0.101					56	0.084	3.69	0.056	0.291	0.195	0.112
18	0.010	0.199					58	0.086	3.77	0.057	0.302	0.212	0.126
19	0.014	0.334					60	0.087	3.84	0.058	0.312	0.229	0.141
20	0.018	0.500					65	0.090	3.97	0.060	0.334	0.266	0.179
22	0.025	0.796					70	0.092	4.08	0.063	0.354	0.299	0.219
24	0.034	1.14					80	0.094	4.25	0.070	0.385	0.356	0.295
26	0.044	1.66					90	0.095	4.32	0.072	0.398	0.396	0.359
28	0.049	1.94	0.007				100	0.095	4.31	0.072	0.402	0.420	0.412
30	0.052	2.13	0.011	0.014			120	0.095	4.30	0.073	0.403	0.455	0.506
32	0.055	2.31	0.021	0.026			150	0.093	4.20	0.072	0.394	0.477	0.589
34	0.058	2.49	0.025	0.054			200	0.090	4.00	0.067	0.361	0.474	0.640
36	0.061	2.66	0.029	0.094	0.004	0.006	250	0.085	3.75	0.063	0.332	0.445	0.626
38	0.064	2.82	0.034	0.122	0.013	0.014	300	0.080	3.48	0.058	0.293	0.409	0.585
40	0.067	2.95	0.038	0.155	0.038	0.022	400	0.070	3.07	0.050	0.246	0.349	0.503
42	0.070	3.07	0.042	0.180	0.060	0.032	500	0.062	2.74	0.044	0.210	0.298	0.433
44	0.072	3.18	0.045	0.199	0.083	0.043	600	0.057	2.47	0.039	0.183	0.262	0.386
46	0.074	3.28	0.048	0.220	0.102	0.052	700	0.053	2.24	0.035	0.161	0.236	0.337
48	0.077	3.36	0.050	0.239	0.124	0.063	800	0.049	2.07	0.032	0.144	0.213	0.301
50	0.079	3.45	0.052	0.256	0.143	0.073	900	0.047	1.92	0.032	0.133	0.196	0.278
52	0.081	3.53	0.054	0.269	0.160	0.085							

Electron energy (eV)	Ion						Electron energy (eV)	Ion					
	SiF_3^{++}	SiF_2^{++}	SiF^{++}	Si^{++}	F^{++}/Si^{+++}	Total		SiF_3^{++}	SiF_2^{++}	SiF^{++}	Si^{++}	F^{++}/Si^{+++}	Total
16						0.003	54	0.010	0.022	0.002			4.37
17						0.107	56	0.012	0.029	0.003			4.52
18						0.209	58	0.013	0.034	0.004			4.66
19						0.348	60	0.015	0.039	0.005	0.001		4.79
20						0.518	65	0.018	0.052	0.010	0.002		5.07
22						0.821	70	0.021	0.062	0.015	0.005		5.32
24						1.17	80	0.025	0.085	0.023	0.010		5.74
26						1.70	90	0.029	0.103	0.031	0.015	0.0001	5.99
28						2.00	100	0.033	0.116	0.038	0.019	0.0007	6.12
30						2.20	120	0.038	0.132	0.048	0.027	0.002	6.32
32						2.41	150	0.040	0.140	0.054	0.034	0.004	6.37
34						2.63	200	0.039	0.139	0.058	0.042	0.006	6.20
36						2.85	250	0.035	0.126	0.056	0.046	0.007	5.84
38						3.07	300	0.032	0.113	0.052	0.045	0.008	5.41
40						3.27	400	0.025	0.093	0.045	0.043	0.009	4.72
42						3.46	500	0.021	0.077	0.039	0.039	0.010	4.16
44	0.001	0.003				3.63	600	0.018	0.067	0.035	0.035	0.010	3.73
46	0.003	0.004				3.79	700	0.016	0.061	0.032	0.033	0.009	3.36
48	0.004	0.007				3.93	800	0.015	0.054	0.028	0.031	0.009	3.08
50	0.006	0.011				4.08	900	0.013	0.046	0.026	0.029	0.008	2.85
52	0.008	0.016				4.23							

lower masses. The intensities of the singly charged ions SiF_2^+, SiF^+, Si^+, and F^+ and the doubly charged ions SiF_3^{++} and SiF^{++} are significantly higher in our spectrum than the corresponding intensities found in the mass spectra in the various databases. The reason for this discrepancy may be the high detection efficiency of our TOFMS for ions with significant excess kinetic energy (see the following). On the other hand, some databases[41,43] reveal somewhat higher relative intensities for the doubly charged ions SiF_2^{++} and Si^{++}. No data on electron beam intensity and target gas pressure are given there to exclude multielectron collisions as a possible source of the disparities.

We carried out qualitative determinations of the excess kinetic energy for all fragment ions by performing a full

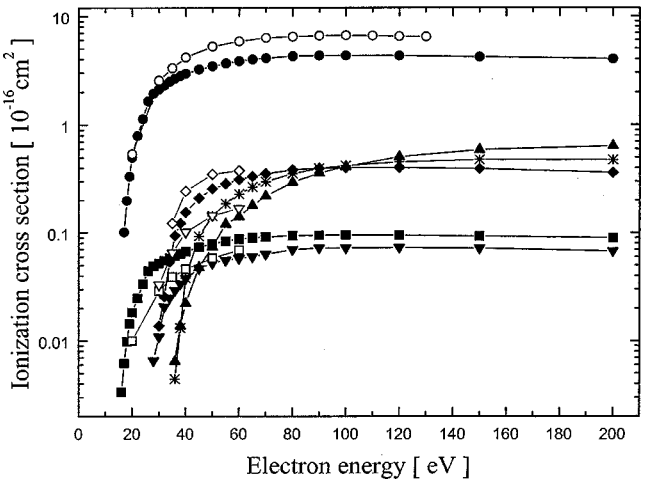

FIG. 4. Absolute partial SiF_4 ionization cross sections for the singly charged ions SiF_4^+/appearance energy: 15.7±0.3 eV (closed squares: present data, open squares: Ref. 13), SiF_3^+/16.5±0.3 eV (closed circles: present data, open circles: Ref. 12), SiF_2^+/25.6±2.3 eV (closed inverted triangles: present data, open inverted triangles: Ref. 13), SiF^+/28.2±2.0 eV (closed diamonds: present data, open diamonds: Ref. 13), Si^+/33.7±2.4 eV (stars: present data), and F^+/34.6±2.2 eV (closed triangles: present data) as a function of electron energy up to 200 eV.

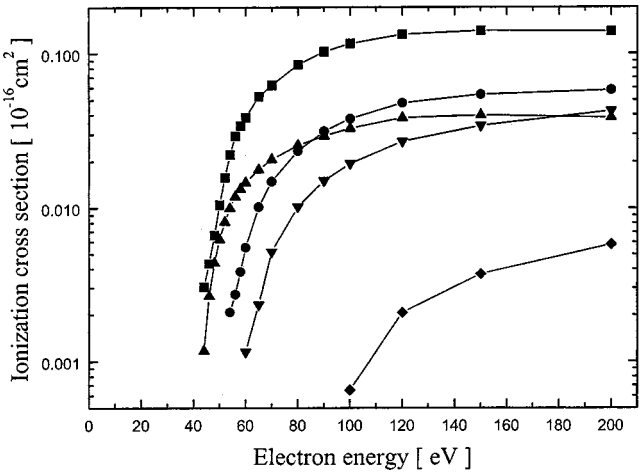

FIG. 5. Present absolute partial (counting) SiF_4 ionization cross sections of the doubly charged ions, SiF_3^{++}/41.2±2.6 eV (triangles), SiF_2^{++}/42.7±2.8 eV (squares), SiF^{++}/51.2±2.7 eV (circles), Si^{++}/55.2±2.9 eV (inverted triangles), and F^{++}/Si^{+++}/80±10 eV (diamonds) as a function of electron energy up to 200 eV.

horizontal sweep of the extracted ion beam using a double-focusing mass spectrometer.[32,33] The results of these measurements are presented in Fig. 3. The shape of the SiF_4^+ parent ion signal is representative of an ion beam with no excess kinetic energy. The shape of the ion signal for the SiF_3^+ fragment ion shows an ion distribution indicative of a small amount of excess kinetic energy. All other ions show beam profiles indicative of a broad distribution of excess kinetic energies as shown for SiF^+ and Si^+ in Fig. 3. We found that the shapes and the widths of the ion beam profiles differed slightly for the various fragment ions. This indicates different excess kinetic energy distributions for the different fragment ions. The doubly charged fragment ions of SiF_4 yield similar results. The ion beam profiles of the doubly charged are compared with the beam profile of the Ar^{++} ions. In general, the doubly charged ions show somewhat narrower beam profiles than the singly charged ions. This finding is not unexpected and confirms the results of previous photoionization studies of SiF_4.[21]

We found no evidence for the thermal decomposition of SiF_4 at the hot surface of the filament used in the electron gun. We detected no traces of fluorine in the mass spectrum and the measured appearance energy for the F^+ ions of 34.6 eV (see Fig. 4) is much higher than the ionization energy of atomic F (17.422 eV, Ref. 44) and the appearance energy of F^+ from F_2 (15.6 eV, Ref. 44). This demonstrates that the entire recorded F^+ ion signal can be attributed to F^+ fragment ions resulting from the dissociative ionization of SiF_4.

The numerical values of the partial ionization cross sections for the formation of singly charged ions, the partial counting ionization cross sections for the formation of doubly charged ions, and the total (charge weighted) ionization cross section as a function of the energy of the ionizing electrons from threshold to 900 eV are given in Table I. The corresponding cross-section curves are shown in Figs. 4–6, for impact energies up to 200 eV. Figure 4 shows the cross sections for all singly charged ions and Fig. 5 depicts the cross-section curves for the doubly charged ions measured as part of this work. The formation of SiF_3^+ fragment ions from SiF_4 is by far the dominant ionization process. The SiF_3^+ cross sections exhibit a maximum around 90 eV with a peak value of 4.32×10^{-16} cm^2. This corresponds to about 77% of the total single ionization cross section of SiF_4 and 72% of the total (charge weighted) SiF_4 ionization cross section. The dominance of the SiF_3^+ partial ionization cross section becomes even more dominant in the low energy region, which is of special interest for low-temperature plasma technology. At 40 eV, SiF_3^+ ions represent 90% of all ions produced by electron impact on SiF_4. The doubly charged fragment ions

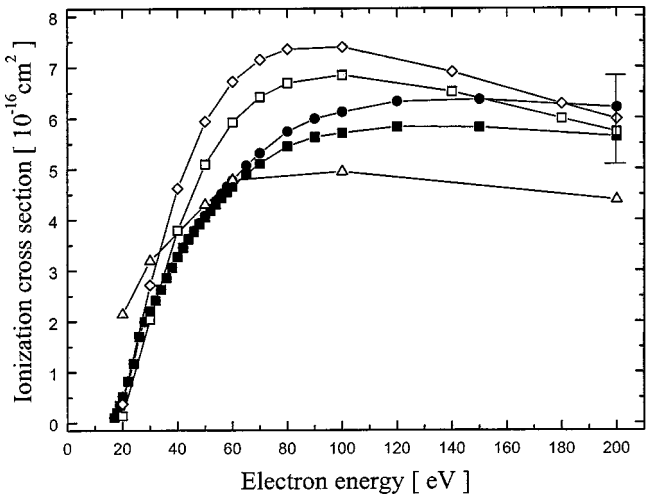

FIG. 6. Absolute total single SiF_4 ionization cross section as a function of electron energy up to 200 eV, present experiment (closed squares) and calculated cross sections using the MAR (open triangles) and the DM formalism with experimental ionization energies (open squares) and with calculated ionization energies (open diamonds). Also shown are the present results of the total (charge-weighted sum of the measured singly and doubly charged ions) ionization cross section (closed circles).

TABLE II. Required constants and quantities for the calculation of the total single ionization cross section of SiF_4 using the DM formalism. MO denotes the molecular orbital, AO refers to the atomic F and Si orbitals. The quantity r_{nl} is the radius of maximum radial density of the atomic subshell characterized by the quantum numbers n and l (column 1 in the tables of Desclaux—Ref. 51), ξ_{nl} refers to the number of atomic electrons in the (n,l) subshell. E_{nl} refers to the ionization energy in the (n,l) subshell and the g_{nl} are appropriately chosen weighting factors (see Ref. 50 for details). The superscripts ''expt'' and ''calc'' designate, respectively, the experimentally determined and calculated ionization energies E_{nl}. Since the product $(E_{nl}\cdot g_{nl})$, the so-called reduced weighting factor, is a constant (Ref. 50), two slightly different sets of weighting factors g_{nl}^{expt} and g_{nl}^{calc} correspond to the two ionization energies E_{nl}^{expt} and E_{nl}^{calc}.

MO	AO	r_{nl} [10^{-9} cm]	ξ_{nl}	E_{nl}^{expt} (eV)	g_{nl}^{expt}	E_{nl}^{calc} (eV)	g_{nl}^{calc}
$(1t_1)^6$	F(2p)	3.812	6.000	16.4	1.8293	14.95	2.006
$(5t_2)^6$	F(2p)	3.812	5.532	17.4	1.7241	16.15	1.857
	F(2s)	4.056	0.102	17.4	1.1494	16.15	1.238
	Si(3p)	1.53	0.348	17.4	1.4378	16.15	1.548
	Si(3s)	9.487	0.018	17.4	0.8046	16.15	0.867
$(1e)^4$	F(2p)	3.812	3.480	18.1	1.6575	16.65	1.802
	Si(3p)	11.53	0.520	18.1	1.3812	16.65	1.501
$(4t_2)^6$	F(2p)	3.812	4.518	19.4	1.5464	18.13	1.655
	F(2s)	4.056	0.378	19.4	1.0309	18.13	1.103
	Si(3p)	11.53	1.104	19.4	1.2887	18.13	1.379
$(5a_1)^2$	F(2p)	3.812	1.194	21.4	1.4019	20.04	1.497
	F(2s)	4.056	0.354	21.4	0.9346	20.04	0.998
	Si(3p)	11.53	0.058	21.4	1.1682	20.04	1.247
	Si(3s)	9.487	0.394	21.4	0.5642	20.04	0.699
$(3t_2)^6$	F(2p)	3.812	0.180	39.3	0.7634	35.62	0.842
	F(2s)	4.056	5.100	39.3	0.5089	35.62	0.561
	Si(3p)	11.53	0.720	39.3	0.6361	35.62	0.702
$(4a_1)^2$	F(2p)	3.812	0.124	40.6	0.7389	36.88	0.813
	F(2s)	4.056	1.578	40.6	0.4926	36.88	0.542
	Si(3s)	9.487	0.298	40.6	0.3448	36.88	0.380

appear above an impact energy of 40 eV. Their absolute cross-section values are comparatively small. The peak value of the most abundant doubly charged ion, SiF_2^{++}, reaches $0.14\times10^{-16}\,cm^2$ at 150 eV impact energy. It is noteworthy that the ion abundances for, respectively, the singly and doubly charged ions are quite different. We found no detectable SiF_4^{++} ion signal. While SiF_3^+ is formed with a comparatively large cross section, we found only a small SiF_3^{++} ion signal. On the other hand, SiF_2^{++} is the doubly charged ion with the largest cross section, whereas SiF_2^+ has the smallest cross section among the singly charged ions and, in fact, the SiF_2^+ cross section is smaller than the SiF_2^{++} cross section for energies above 70 eV. For all other fragments, the cross sections for formation of the doubly charged ion are about one order of magnitude smaller than those for the formation of the singly charged ion. A very small ion signal was detected around a mass-to-charge (m/z) ratio of 9–10, which we attribute to F^{++} and Si^{+++}, because a measurement with the TOFMS in the high-resolution reflection mode clearly showed two separate peaks.

The measured appearance energies for the various ions with their respective uncertainties are given in the figure captions of Figs. 4 and 5. The appearance energies were obtained from a linear extrapolation of the ion signal in the case of the singly charged ions and from a square-root extrapolation in the case of the doubly charged ions. Our values are in good agreement with previously reported electron impact data from McDonald *et al.*[45] for SiF_x^+ $(x=1-4)$ and with photoionization data from Imamura *et al.*[21] for Si^+, F^+, and the doubly charged ions. The appearance energies for SiF_2^+, SiF^+, and Si^+ given by Nakano and Sugai [13] are lower by 3 eV, but their values for SiF_4^+ and SiF_3^+ agree with the present data. It is noteworthy that we observed extended curvatures in the near-threshold regions for all the light fragment ions, which significantly exceeded the curvature attributable to the energy spread in the electron beam. In almost all cases, this extended curvature determined the quoted uncertainty in the respective appearance energy determination. We attribute this curvature to the presence of different ionization channels[13] and to the generation of fragment ions with broad distributions of excess kinetic energy.

Also shown in Fig. 4 are the only previously measured partial ionization cross sections of SiF_4, the cross sections for SiF_3^+,[12] and the cross sections for SiF_4^+, SiF_2^+, and SiF^+[13] which were calibrated on the basis of the SiF_3^+ cross section of Ref. 12. The SiF_3^+ cross section of Ref. 12 increases more rapidly than our cross section for impact energies above 30 eV and exceeds our cross section by about 50%. A comparison of our results with the data of Nakano and Sugai[13] reveals that for all impact energies our SiF_4^+ cross section is higher (up to 26%) and our SiF_2^+ and SiF^+ cross sections are lower (up to 65% and 18%, respectively) than their results.

The experimentally derived total (charge weighted) SiF_4 ionization cross section (the last column in Table I) is shown in Fig. 6 together with the total single SiF_4^+ ionization cross section (the sum of all partial ionization cross sections leading to the formation of a singly charged product ion) for electron energies up to 200 eV. Also shown are three calculated total single ionization cross-section curves using, on the one hand, the semiempirical modified additivity rule (MAR) and, on the other hand, the more rigorous semiclassical Deutsch–Märk (DM) formalism in two variants. The MAR results are taken from Ref. 46 where the authors describe the MAR concept and discuss in detail the calculation of the ionization cross sections for all four SiF_x $(x=1-4)$ compounds. The DM formalism was originally developed for the calculation of atomic ionization cross sections[47] and subsequently applied to molecules.[48,49] A comprehensive discussion of the DM formalism and of its application to more than 30 molecules and free radicals can be found in a recent review[50] to which we refer the reader for further details. It suffices to say here that the application of the DM formalism to a molecule requires a Mulliken population analysis or an equivalent method that expresses the molecular orbitals in terms of atomic orbitals of the constituent atoms and determines relevant atomic orbital populations. Table II includes all quantities that are required for the DM calculation of the SiF_4 total single ionization cross section. The two DM calculations refer to calculations using either a set of experimentally determined ionization energies[21,22] or a set of calculated ionization energies.[22]

Figure 6 shows the comparison of the experimentally determined and the calculated cross sections. The MAR yields a calculated cross section that is higher than the experimental data for all energies below about 60 eV (by as much as 300% at 20 eV) and falls below the experimental data above this energy (by about 20% at 200 eV). In the case of DM formalism, the ionization cross-section curve derived with the calculated ionization energies exceeds the calculated curve based on the experimental ionization energies in the entire energy range. There is good agreement between the experimentally determined cross section and both DM calculations for impact energies up to about 30 eV. For higher impact energies, the calculated cross-section curves increase more rapidly than the experimental values and lie systematically above the experimental data. The maximum deviation of about 25% (experimental ionization energies) and 45% (calculated ionization energies) are found in the energy range from 50 to 60 eV. At higher impact energies, the agreement between the calculated and measured cross sections improves again. At 200 eV, the deviation between the two calculated curves and the measured data has reached a level of about 5%. In view of the overall uncertainty of about $\pm 15\%$ in the measured partial ionization cross section, we conclude that this level of agreement between experiment and calculation is quite satisfactory, in particular with the DM calculation based on the experimentally determined ionization energies.

IV. CONCLUSIONS

We measured the absolute partial electron impact ionization cross sections for the SiF_4 molecule using a time-of-flight mass spectrometric technique. The mass spectrum at 70 eV is in good agreement with known mass spectral cracking patterns of SiF_4 for the higher ion masses. Differences with previously published data at lower ion masses, in particular for SiF_x^+ $(x=0-2)$ and F^+ can be explained in terms of the excess kinetic energy of these fragment ions, which may have affected the earlier measurements. Our technique has a very high extraction and detection efficiency for energetic ions. A complete set of the absolute ionization cross sections for the formation of singly and doubly charged ions from SiF_4 was determined with an overall uncertainty of $\pm 15\%$. These results represent the first complete set of ionization cross-section data regarding the electron impact ionization of SiF_4. The experimental total single ionization cross section is in reasonable agreement with semiempirical and semiclassical calculations. The absolute cross-section values measured here are indispensable for a microscopic understanding and a detailed modeling of the plasma chemical processes in SiF_4-containing plasmas and in other plasmas containing F-bearing molecules in the feed gas mixtures that are used to etch Si and SiO_2. The data presented here are also important for the critical evaluation of mass spectrometric plasma diagnostics data.

ACKNOWLEDGMENTS

This work was partially supported by the DAAD (971219-R). One of us (K.B.) acknowledges partial financial support from the Division of Chemical Sciences, Office of Basic Energy Sciences, Office of Science, U.S. Department of Energy. The authors are grateful for technical assistance provided by U. Haeder.

[1] D. L. Flamm and V. M. Donnelly, Plasma Chem. Plasma Process. **1**, 317 (1981).
[2] H. F. Winters and F. A. Houle, J. Appl. Phys. **54**, 1218 (1983).
[3] Y. Matsumi, S. Toyoda, T. Hayashi, M. Miyamura, H. Yoshikawa, and S. Komiya, J. Appl. Phys. **60**, 4102 (1986).
[4] M. Sugewara, *Plasma Etching: Fundamentals and Applications* (Oxford University Press, Oxford, 1988).
[5] B. D. Pandt and U. S. Tandon, Plasma Chem. Plasma Process. **19**, 545 (1999).
[6] B. Lee, L. J. Quinn, P. T. Baine, S. J. N. Mitchell, B. M. Armstrong, and H. S. Gamble, Thin Solid Films **337**, 55 (1999).
[7] A. M. Ali, T. Inokuma, Y. Kurata, and S. Hasegawa, Jpn. J. Appl. Phys., Part 1 **38**, 6047 (1999).
[8] T. R. Hayes, R. Shul, F. A. Biaocchi, and R. S. Freund, J. Chem. Phys. **88**, 823 (1987).
[9] T. R. Hayes, R. J. Shul, F. A. Biaocchi, R. C. Wetzel, and R. S. Freund, J. Chem. Phys. **89**, 4035 (1987).
[10] R. J. Shul, T. R. Hayes, F. A. Biaocchi, and R. S. Freund, J. Chem. Phys. **89**, 4042 (1987).
[11] R. S. Freund, R. C. Wetzel, R. J. Shul, and T. R. Hayes, Phys. Rev. A **41**, 3575 (1990).
[12] H. U. Poll and J. Meichsner, Contrib. Plasma Phys. **27**, 359 (1987).
[13] T. Nakano and H. Sugai, J. Phys. D **26**, 1909 (1993).
[14] N. Abramzon, T. Raynor, K. E. Martus, and K. Becker, Bull. Am. Phys. Soc. (in press).
[15] G. W. Karwasz, R. S. Brusa, A. Zecca, P. Mozejko, P. Kasperski, and Cz. Szmytkowski, Chem. Phys. Lett. **284**, 128 (1998).
[16] R. Nagpal and A. Garscadden, Appl. Phys. Lett. **68**, 2189 (1996).
[17] J. F. M. Aarts, Chem. Phys. **101**, 105 (1986).

[18] I. Iga, M. V. V. S. Rao, S. K. Srivastava, and J. C. Nogueira, Z. Phys. D: At., Mol. Clusters **24**, 111 (1992).
[19] M. Suto, X. Wang, L. C. Lee, and T. J. Chuang, J. Chem. Phys. **86**, 1152 (1987).
[20] K. Kameta, M. Ukai, T. Numazawa, N. Terazawa, Y. Chikahiro, N. Kouchi, Y. Hatano, and K. Tanaka, J. Chem. Phys. **99**, 2487 (1993).
[21] T. Imamura, C. E. Brion, I. Koyano, T. Ibuki, and T. Masuoka, J. Chem. Phys. **94**, 4936 (1991).
[22] H. Ishikawa, K. Fujima, H. Adachi, E. Miyauchi, and T. Fujii, J. Chem. Phys. **94**, 6740 (1991).
[23] M. E. Wecker and P. B. Armentrout, J. Chem. Phys. **88**, 6898 (1988).
[24] B. L. Kickel, E. R. Fisher, and P. B. Armentrout, J. Phys. Chem. **97**, 10198 (1993).
[25] E. W. Ignacio and H. B. Schlengel, J. Phys. Chem. **96**, 1620 (1992).
[26] S. P. Frigo, J. K. Simons, and R. A. Rosenberg, J. Chem. Phys. **103**, 10356 (1995).
[27] S. P. Frigo, J. K. Simons, and R. A. Rosenberg, J. Chem. Phys. **103**, 10366 (1995).
[28] V. Tarnovsky, A. Levin, K. Becker, R. Basner, and M. Schmidt, Int. J. Mass Spectrom. Ion Processes **133**, 175 (1994).
[29] R. Basner, M. Schmidt, H. Deutsch, V. Tarnovsky, A. Levin, and K. Becker, J. Chem. Phys. **103**, 211 (1995).
[30] R. Basner, M. Schmidt, and H. Deutsch, Contrib. Plasma Phys. **35**, 375 (1995).
[31] R. Basner, R. Foest, M. Schmidt, F. Sigeneger, P. Kurunczi, K. Becker, and H. Deutsch, Int. J. Mass Spectrom. Ion Processes **153**, 65 (1996).
[32] R. Basner, M. Schmidt, V. Tarnovsky, and K. Becker, Int. J. Mass Spectrom. Ion Processes **171**, 83 (1997).
[33] R. Basner, R. Foest, M. Schmidt, K. Becker, and H. Deutsch, Int. J. Mass Spectrom. Ion Processes **176**, 245 (1998).
[34] R. Basner, M. Schmidt, K. Becker, and H. Deutsch, *Electron Impact Ionization of Organic Silicon Compounds*, in Advances in Atomic, Molecular, and Optical Physics Vol. 43, edited by M. Inokuti and K. Becker (Academic, New York, 1999), pp. 147–185.
[35] R. Basner, M. Schmidt, V. Tarnovsky, K. Becker, and H. Deutsch, Thin Solid Films **374**, 291 (2000).
[36] C. Ma, C. R. Sporleder, and R. A. Bonham, Rev. Sci. Instrum. **62**, 909 (1991).
[37] H. C. Straub, P. Renault, B. G. Lindsay, K. A. Smith, and R. F. Stebbings, Phys. Rev. A **52**, 1115 (1995).
[38] D. Rapp and J. Englander-Golden, Chem. Phys. **43**, 1464 (1965).
[39] V. Tarnovsky and K. Becker, Z. Phys. D: At., Mol. Clusters **22**, 603 (1992).
[40] M. R. Bruce and R. A. Bonham, Z. Phys. D: At., Mol. Clusters **24**, 149 (1992).
[41] NIST/EPA/NIH Mass Spectral Database, V4/5 (http://webbook.nist.gov/chemistry).
[42] *Eight Peak Index of Mass Spectra*, 2nd ed. (Mass Spectrometry Data Center, Aldermaston, 1974).
[43] *Compilation of Mass Spectral Data*, 2nd ed., edited by A. Cornu and R. Massot (Heyden, London, 1975).
[44] H. M. Rosenstock, K. Draxl, B. W. Steiner, and J. T. Herron, J. Phys. Chem. Ref. Data Suppl. **6**, I-344 (1977).
[45] J. D. McDonald, C. H. Williams, J. C. Thompson, and J. L. Margrave, Adv. Chem. Ser. **72**, 261 (1968).
[46] H. Deutsch, K. Becker, R. Basner, M. Schmidt, and T. D. Märk, J. Phys. Chem. **106**, 8819 (1998).
[47] H. Deutsch and T. D. Märk, Int. J. Mass Spectrom. Ion Processes **79**, R1 (1987).
[48] H. Deutsch, C. Cornelissen, L. Cespiva, V. Bonacic-Koutecky, D. Margreiter, and T. D. Märk, Int. J. Mass Spectrom. Ion Processes **129**, 43 (1993).
[49] H. Deutsch, T. D. Märk, V. Tarnovsky, K. Becker, C. Cornelissen, L. Cespiva, and V. Bonacic-Koutecky, Int. J. Mass Spectrom. Ion Processes **137**, 77 (1994).
[50] H. Deutsch, K. Becker, and T. D. Märk, Int. J. Mass. Spectrom. **197**, 37 (2000).
[51] J. P. Desclaux, At. Data Nucl. Data Tables **12**, 325 (1973).